Technical Report

Developing Solutions to Improve the Functionality of Chassis Parts

Kenichiro OHTSUKA*
Manabu WADA
Ryo URUSHIBATA
Yuki KITAHARA
Eiji ISOGAI
Hikaru YUZAWA
Ryo TABATA
Ryoya YAMAOKA

Abstract

As we promote the electrification of chassis parts, we are developing a set of advanced materials and solutions to provide advantage in part weight, cost, and life cycle GHG emissions. We introduce a development example of a lower arm and subframe that weigh the same as aluminum while meeting the part requirements of electric vehicles by applying Nippon Steel Corporation's 980 MPa-grade high tensile steel, forming method, and developed structure. We also introduce a development example of a steel tube trailing arm, at a lower cost than those made using conventional steel tube forming methods in order to accommodate the application of steel tube parts to rear suspensions with the aim of increasing the amount of battery capacity installed.

1. Introduction

In recent years, automobiles have been rapidly electrified to address global warming and air pollution issues. However, electrification has brought challenges for automakers, such as increased vehicle weight, higher costs, and stricter crash requirements to protect batteries. To tackle these challenges, the demand for applying high-strength steel sheets to chassis components has been growing among automakers. Compared to aluminum materials, the application of high-strength steel sheets offers advantages in terms of cost and CO_2 emissions (LCA)[1]. By mastering the use of steel, it is possible to achieve weight reduction, cost efficiency, and LCA performance simultaneously. To meet these requirements and contribute to solving the challenges of vehicle electrification, Nippon Steel Corporation has proposed NSafe™-AutoConcept ECO[3]. Within this concept, we have been developing chassis components with advanced steel materials and integrated solutions to achieve component weights equivalent to aluminum.

For arm-link components in chassis systems, we are promoting the development of hot-rolled 980 MPa-grade high-formability steel sheets (980HF), forming methods, and structural design techniques to address the reduced design flexibility and performance degradation caused by decreased formability due to high-strength steel application. For subframes, we are developing GA980EA (energy absorption) material, which offers excellent crash fracture resistance, along with manufacturing methods that reduce the number of parts and welding points, aiming to improve crash performance and reduce costs. In addition, for rear suspension systems, steel tubes are sometimes applied to achieve space-saving designs that allow for increased battery installation capacity. To address this, we are developing low-cost tube forming methods using 980 MPa-grade high-strength steel tubes.

This report introduces development examples of a front lower arm and a front subframe that meet the requirements of electric vehicles with weights equivalent to aluminum, as well as a trailing arm using steel tubes that achieves lower costs compared to conventional designs.

2. Development of a Lightweight Front Lower Arm

2.1 Development background

As a representative chassis component, the front lower arm requires high strength for its functional performance. Consequently, the application of high-strength steel sheets is expected to advance to meet the stricter requirements accompanying electrification. However, as steel sheet strength increases, ductility and hole-expan-

* Senior Manager, Head of Section, Integrated Steel-Solution Research Lab.-I, Steel Research Laboratories
20-1 Shintomi, Futtsu City, Chiba Pref. 293-8511

sion properties decrease, leading to a tendency for the wall height of the curved section—subjected to stretch flange deformation—to decrease (**Fig. 1**). This reduction in wall height significantly lowers fatigue durability, becoming a barrier to further component weight reduction. In other words, increasing the height of the curved section enables further weight reduction of the component. For example, in the case of the front lower arm shown in **Fig. 2**, thinning (lightweighting) increases stress concentration at the edge of the curved section, which can cause fatigue failure under cyclic loading. Conversely, increasing the height of the curved section allows for a reduction in stress concentration even after thinning, compared to before thinning.

To increase the forming height of the curved section, conventional methods generally employ reducing sheet thickness during forming or controlling material flow to ensure the material's fracture limit is not exceeded.[2–4] In contrast, the sheet thickness compression method, a forming technology developed by Nippon Steel, enables increased forming height of curved sections by enhancing the material's fracture limit. Combining this sheet thickness compression method with the hot-rolled 980 MPa-grade high-formability steel sheet (980HF) shown in **Table 1** achieved an unprecedented balance of increased forming height for curved sections and high strength. Furthermore, utilizing topology optimization[5] for the optimal placement of reinforcing members, a lower arm was developed that satisfies the component requirements for C-segment electric vehicles while matching the weight of aluminum parts.

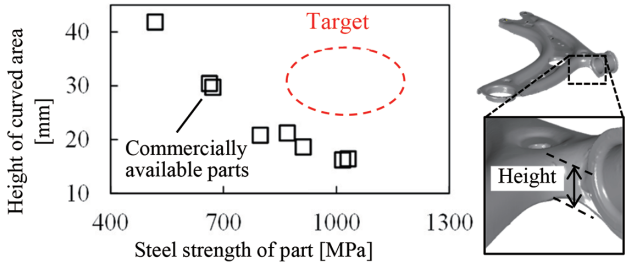

Fig. 1 Relationship between material strength and height of stretch-flange

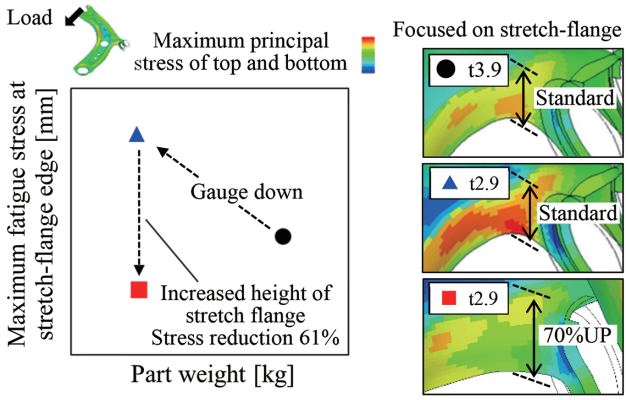

Fig. 2 Relationship between part weight and fatigue stress

Table 1 Mechanical properties of 980HF

	YP (MPa)	TS (MPa)	EL (%)	λ (%)
980HF	843	1 006	13	55

2.2 Sheet thickness compression method

Previous studies have reported that applying hydrostatic pressure during tensile testing of steel round bars improves ultimate deformation capacity (**Fig. 3**).[6] Similarly, in the sheet thickness compression method, forming while applying pressure near the edge of the stretch flange forming section using the holder and die enables increased hydrostatic pressure near the edge (**Fig. 4**). Furthermore, forming while applying pressure in the sheet thickness direction disperses deformation and suppresses local necking. **Figure 5** shows the press process (six steps total) for the front lower arm incorporating this sheet thickness compression method.

- Step 1: Shearing of the curved section using a die (punching clearance CL/t=11%).
- Step 2: Forming of the curved section using the sheet thickness compression method (leaving the flange).
- Step 3: Shearing of the flange of the curved section using a die (punching clearance CL/t=11%).
- Step 4: Forming of the curved section again using the sheet thickness compression method.
- Step 5: Hole drilling on the burring section.

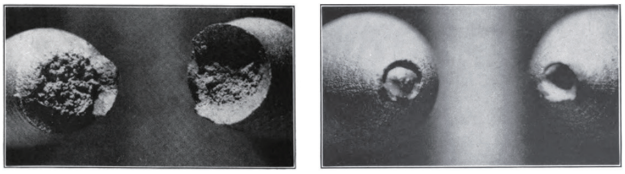

(a) Fracture of specimen broken at atmospheric pressure

(b) Fracture of specimen broken under high hydrostatic pressure

Fig. 3 Effect of hydrostatic pressure on ductility[6]

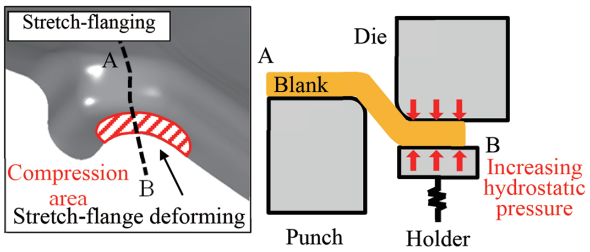

Fig. 4 Sheet thickness compression forming method

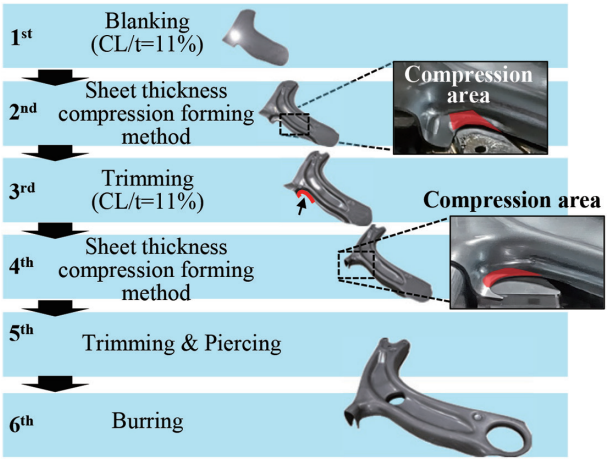

Fig. 5 Sheet thickness compression forming method applied to press molding process of front lower arm

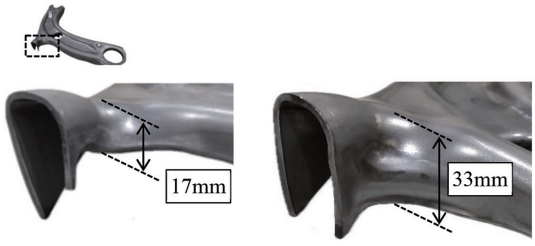

Fig. 6 Results of press forming test

- Step 6: Burring process.

Figure 6 shows the forming test results for the front lower arm. While the conventional part had a maximum height of 17 mm for the curved section, applying the sheet thickness compression method increased the maximum height to 33 mm.

2.3 Structural optimization

Electric vehicles have higher vehicle weights than internal combustion engine vehicles, demanding higher component performance (crashworthiness, stiffness, fatigue durability) from the front lower arm. Solid cross-section structures or welded closed-section structures (two upper/lower parts) easily ensure strength but result in over-performance for crashworthiness and rigidity, reducing weight efficiency. In contrast, partially optimizing the placement of open and closed sections according to performance requirements yields components with superior weight efficiency. Therefore, to optimize section placement, nonlinear structural optimization methods were used to extract key points for section design.

Figure 7 illustrates the optimal placement of reinforcement members, focusing on the component's strength characteristics (retraction force). Using a lower arm with an open section structure made of 980HF (with sheet thickness compression method applied to the curved section) as the base, nonlinear topology optimization was performed with the inner section as the design space. The generated structure suggested reinforcement is needed in three areas: ① near the ball joint, ② near the stretch flange forming section, and ③ near the burring section. In the unreinforced structure, loading causes deformation to concentrate in areas ① and ②. In contrast, the closed-section structure exhibits smaller overall deformation and higher stiffness. By incorporating reinforcing members at locations ①, ②, and ③, deformation is distributed throughout the entire component. **Figure 8** shows the strength characteristics of the developed component structure. The developed component structure was found to exhibit superior performance compared to the closed-section structure in terms of weight efficiency for retraction force. Although omitted in this report, it also satisfied the component performance requirements for C-segment electric vehicles, including collision performance.

2.4 Advantages of the developed structure

Figure 9 shows a photograph of the developed front lower arm prototype. **Figure 10** demonstrates the advantages of the developed product over the C-segment aluminum front lower arm in terms of CO_2 emissions from LCA and part cost. Calculations indicate the developed lower arm achieves the same weight as aluminum (2.2 kg), reduces CO_2 emissions by 61%, and enables a 65% reduction in part cost. By developing components using a combination of advanced steel materials, forming technologies, and structural design

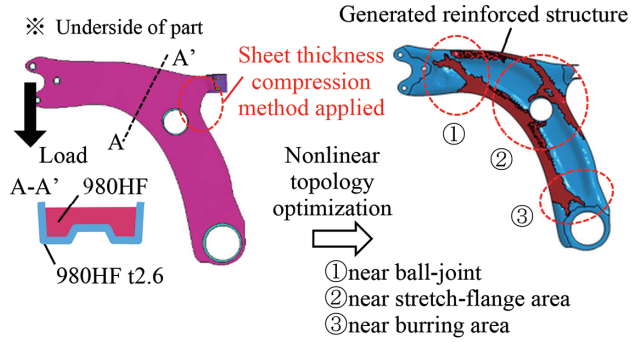

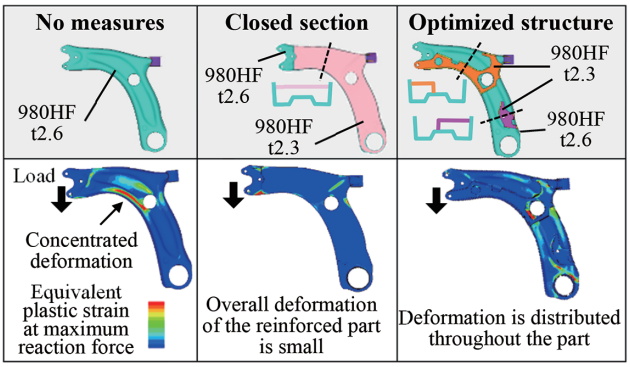

Fig. 7 Optimization of reinforcement structure (CAE analysis)

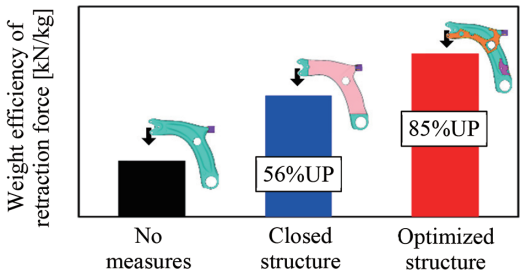

Fig. 8 Crash performance of the developed structure (CAE analysis)

Fig. 9 Developed lower arm

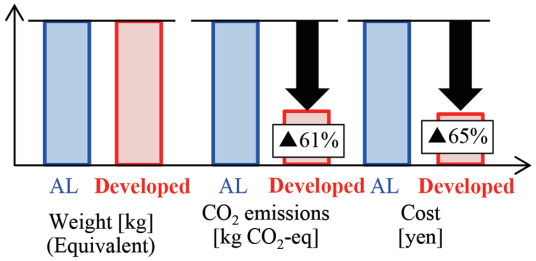

<Electricity cost> Mileage: 100,000 km, Region: Japan (2018)
Rate of non-fossil fuels: 23%

Fig. 10 Comparison of weight, CO_2 emission, cost to aluminum part

techniques, we have developed a steel lower arm component that outperforms aluminum parts. This development methodology is applicable not only to lower arms but also to components with stretch flange sections, enabling its expansion to other parts.

3. Development of a Low-Cost, Mass-Producible Steel Tube Trailing Arm

3.1 Development background

Automotive suspensions exist in various configurations. Among them, the torsion beam suspension is widely used in high-volume vehicles such as kei cars, compact cars, and minivans. Employed as a rear suspension, it consists of a trailing arm connecting the wheel axle to the body, a coil spring, and a torsion beam linking the left and right arms. Compared to other suspension systems, the torsion beam offers advantages of simplicity, light weight, and low cost. However, for electric vehicles, the placement of components such as motors and batteries requires three-dimensionally curved trailing arms to enhance design flexibility under the vehicle floor.

The trailing arm must ensure strength and rigidity along its entire length. Considering weight reduction, the entire component is often designed as a closed-section structure. One method for forming this closed section is the sandwich panel structure, created by arc welding two components obtained by press forming steel sheets. However, the increased complexity of component structures due to electrification, as mentioned earlier, leads to significant stretch flange and shrink flange deformation, demanding high formability. Furthermore, since two curved components must be arc welded together, dimensional accuracy must be ensured by accounting for springback. In contrast, using steel tubing—which is inherently a closed-section structure—as the raw material eliminates the need for forming processes to create the closed section and for arc welding, potentially reducing part manufacturing costs.

Trailing arms are often designed with a rectangular cross-section to facilitate connection with other components. Processing steel tubing into a curved part with a rectangular cross-section requires separate bending and cross-section forming operations. The most widely used bending method is rotary draw bending.[7] Rotary draw bending, capable of bending even small radii, is widely adopted in production. This process involves bending while restrained by multiple dies, which is advantageous for preventing buckling on the inside of the bend.

Various section forming techniques exist, but tube hydroforming (THF) is a processing technology that saw vigorous research and development in the automotive field starting in the 1990s.[8] THF enables forming the part section without buckling by combining internal pressure and axial pressing, making it an exceptionally superior processing method from the perspective of part design freedom. To achieve three-dimensionally curved shapes, a method is used where a blank tube, pre-bent using rotary draw bending, is then section-formed via THF. This is because bending after section forming generally makes the section prone to deformation or buckling. On the other hand, THF has a long cycle time, making it suitable for low-volume production.

3.2 Press bending with cross-sectional deformation of steel tube

To enable mass production of three-dimensionally curved closed-section parts, Nippon Steel developed the press bending method with cross-sectional deformation of steel tube (**Table 2**),[9] a forming technology that simultaneously performs bending and cross-sectional forming on steel tubes. This method is applicable to

Table 2 Comparison of conventional and developed methods

Method	Conventional		Developed
	Pre-forming and press bending	Rotary draw bending and THF	Cross-sectional deformation press bending
Overview	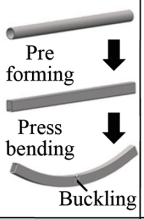	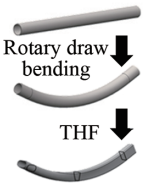	
Productivity	○	×	○
Shape flexibility	×	○	△ Uniform cross section
Shape fixability	△	○	○
Equipment cost	○	×	○
Process-saving	×	×	○

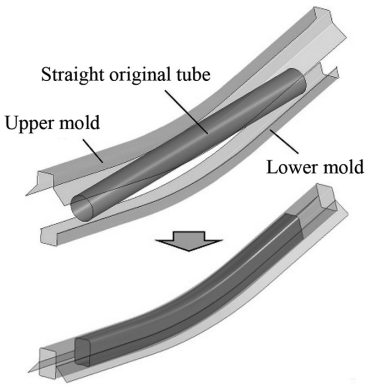

Fig. 11 Die configuration for sectional deformation press bending

conventional presses. It bends the blank tube using upper and lower dies while performing section deformation, thereby distributing the deformation and enabling forming without buckling (**Fig. 11**). Consequently, this method can be considered a process-saving technique suitable for mass production. Furthermore, combining it with rotary draw bending can increase achievable bending radii. Additionally, the die face shape can alter the cross-sectional profile along the tube axis. While the cross-sectional circumference of the part must remain nearly constant, combining it with other processes, such as flaring the tube ends, allows adaptation to variations in cross-sectional circumference.

CAE analysis compares the deformation behavior between conventional press bending and the cross-section deformation press bending method (**Fig. 12**). Here, the base tube has a strength of 980 MPa-grade, an outer diameter of φ40 mm, and a wall thickness of 1.6 mm. The final part shape is formed with a cross-section of 40 mm × 30 mm, a rectangular cross-section structure, an inner bending radius of 800 mm, and a bending angle of 20°. The cross-section deformation press bending method forms the raw tube in a single operation, whereas the conventional method assumes bending a preformed rectangular tube (straight tube) with a rectangular cross-section (40 mm × 30 mm).

Figure 12 shows the axial strain distribution in the tube after processing. In the conventional method bending a rectangular tube, buckling occurs on the bend inside, as shown in Fig. 12 (a). This is

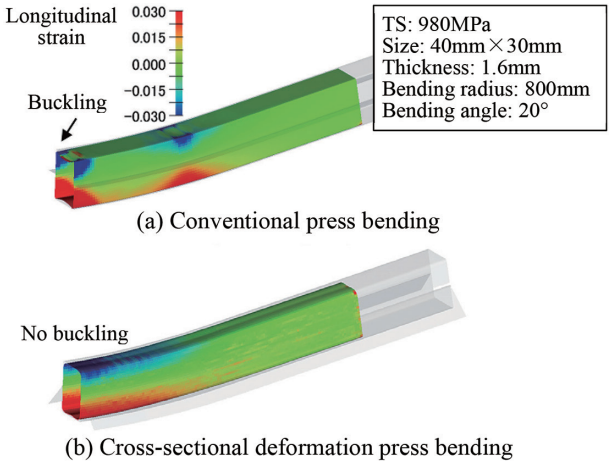

Fig. 12 Comparison of shapes after processing by conventional method and sectional deformation press bending

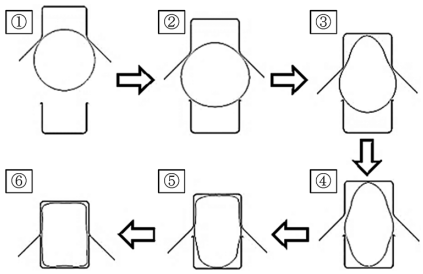

Fig. 13 Cross-sectional shape of the center of the pipe axis due to cross-sectional deformation press bending

because the bend inside is compressed axially by the bending deformation, causing localized out-of-plane deformation. In contrast, the cross-section deformation press bending method, which bends the blank tube, does not exhibit the buckling seen in conventional methods, as shown in Fig. 12(b). This is because simultaneous bending and cross-sectional processing disperses the compressive deformation on the inside of the bend along the tube axis, suppressing buckling.

To examine the change in cross-sectional shape during forming with the cross-section deformation press bending method, the cross-sectional shape at the center of the tube axis is illustrated (**Fig. 13**). The blank tube first contacts the upper die. A guide mechanism provided in the upper die allows the blank tube to flow smoothly into the upper die cavity (① to ③). Subsequently, material also flows into the lower die cavity, and axial bending is nearly complete (④). Then, as the upper die descends to the bottom dead center, a rectangular cross-section is formed (⑤), and the process is completed (⑥). From the above, it can be seen that during bending, the inner side of the bend, which undergoes compressive deformation in the tube axial direction, has a circular cross-section. Compared to conventional methods where a rectangular cross-section is preformed, this results in higher surface rigidity, making buckling less likely to occur.

Although omitted in this report, comparison with the change in bending angle after springback (theoretical solution) for a plain tube subjected to simple bending revealed that applying the cross-section deformation press bending method results in a smaller change in bending angle after springback. This is thought to be due to the dispersion of deformation along the tube axis. The cross-section deformation press bending method enables forming without defects such as buckling, even when using 980 MPa-grade high-strength steel tubes. It also achieves greater section design freedom and dimensional accuracy compared to conventional methods.

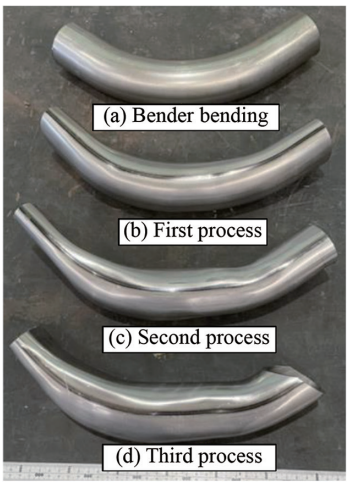

Fig. 14 Trailing arm

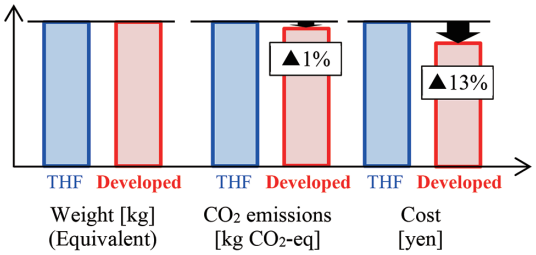

Fig. 15 Comparison of weight, CO_2 emission, cost to THF

An example of applying the cross-section deformation press bending method to the forming process of a trailing arm is introduced. **Figure 14** shows a prototype trailing arm. The base tube was STKM13B with an outer diameter of φ60.5 mm and a wall thickness of 2.3 mm. After rotary draw bending, the part was processed using a three-step cross-section deformation press bending process. The results confirmed that the formed part could be produced with a good shape without buckling or dents.

3.3 Advantages of the developed method

Figure 15 shows the advantages of the developed part over THF in terms of CO_2 emissions in the LCA and part cost. Calculations indicate that the developed part has equivalent weight to THF, 1% lower CO_2 emissions, and a 13% reduction in part cost due to improved productivity.

4. Development of Steel Subframe

4.1 Development background

The subframe of electric vehicles is required to function as a load path and energy-absorbing component during collisions due to the increased vehicle weight and lower center of gravity resulting from battery installation. Furthermore, unlike conventional internal combustion engine vehicles,[10] the mounting method for the power unit in electric vehicles differs significantly. Consequently, a "rectangular frame" configuration equipped with longitudinal and lateral beams to accommodate the motor's center-of-gravity mounting is expected to become mainstream.[11]

Currently, the primary material for subframes is steel, typically fabricated through sheet metal stamping and welded assembly. However, in response to the aforementioned changes, mass-produced vehicles increasingly adopt highly integrated subframe structures utilizing aluminum die-casting and extruded aluminum components. These designs achieve weight reduction while maintaining performance by integrating functional components through die-casting and extrusion, thereby significantly reducing overall weight, part count, and weld length.

Even for steel subframes, there remains a strong demand for cost-effective designs that minimize weight, part count, and weld length. In this study, we developed a front subframe structure for electric vehicles that employs our proprietary steel forming process to achieve a high degree of component integration. This approach ensures structural performance while substantially reducing weight, part count, and weld length.

4.2 Features of the developed front subframe structure and process

The developed front subframe (**Fig. 16**) incorporates components manufactured using the following Nippon Steel proprietary forming methods:

① Front cross member using NSafe™-FORM-SS (Shear Forming Method)[12–14)]

② NSafe™-FORM-LT (Free Bending Method) + Spot TWB for side members and rear cross members[14–16)]

③ Crash box utilizing steel tubing or cross-section deformation press bending method

Details regarding the above processes (①–③) are described below:

① Front cross member using NSafe™-FORM-SS (Shear Forming Method)

The front cross member is positioned forward of the subframe and extends in the vehicle width direction. It ensures rigidity and collision performance, maintains body attachment points, and supports the arms. Nippon Steel's proprietary NSafe™-FORM-SS (Shear Forming Method) is employed to integrally form a shape with a raised body attachment point. Furthermore, the arm support section is integrated into the front cross member. By incorporating the body mounting points and arm support sections—typically separate components in conventional structures—into the front cross member, the number of parts and welding length are reduced (**Fig. 17**). Additionally, GA980 EA steel sheet (t=1.8 mm) is used for this component, achieving thin-walled, lightweight construction while ensuring strength and energy absorption performance.

② NSafe™-FORM-LT (Free Bending Method) + Spot TWB for side members and rear cross members

The side members and rear cross members, which are key components forming the subframe, are integrally formed into a U-shape using NSafe™-FORM-LT (Free Bending Method) and spot TWB. The spot TWB process involves pre-bonding blanks via spot welding before cold forming. This method enables integration of the U-shaped member without compromising yield. Furthermore, integrating the side member and rear cross member reduces the number of parts. For the side member section, NSafe™-FORM-LT (Free Bending Method) is used to form the pocket shape as a single piece (**Fig. 18**). GA980 EA steel sheet (t=2.0 mm) is used for the side member, achieving thin-walled, lightweight construction while ensuring sufficient strength.

③ Crash box utilizing steel tubing or cross-section deformation press bending method

The crash box is a component extending longitudinally at the front end of the subframe. It absorbs energy during the initial to mid-collision phase by undergoing axial crushing deformation. This component employs formed steel tubing to reduce part count and welding length. The steel tube used for this component is 780 MPa-grade (t=1.8 mm) and is mounted on the high-rigidity section of the front cross member. During a collision, axial compression deformation of this component ensures sufficient energy absorption performance. Furthermore, depending on the layout and performance requirements, it is possible to consider forming components with flattened or bent shapes using press bending for section deformation (**Fig. 19**).

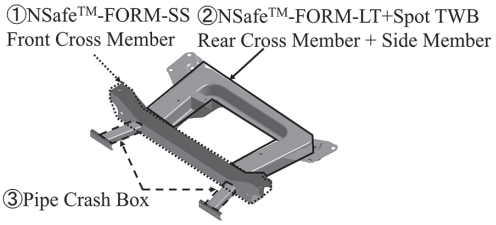

Fig. 16 Developed front subframe

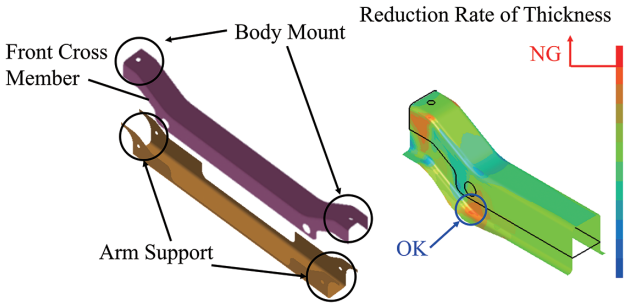

Fig. 17 Development method of front cross member

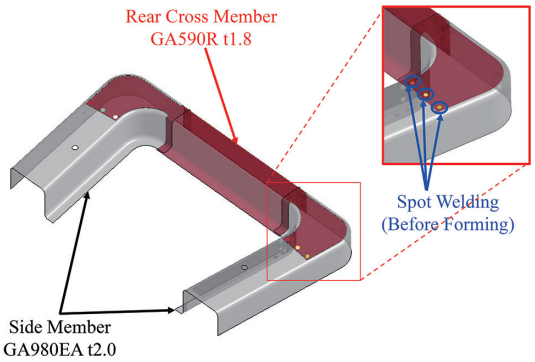

Fig. 18 Side members and cross members applying development methods

4.3 Performance verification

The developed subframe targeted performance equal to or exceeding that of the aluminum front subframe, which was set as the benchmark for this study.

The developed front subframe ensures energy absorption equivalent to or greater than the aluminum front subframe throughout the entire stroke range, as demonstrated by the component collision analysis shown in **Fig. 20**.

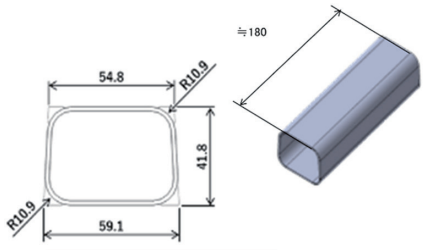

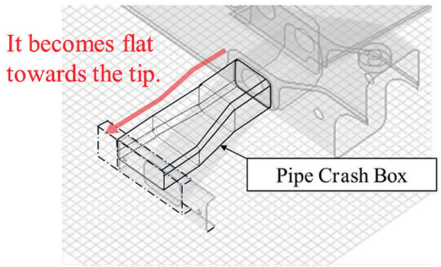

Fig. 19 Steel pipe utilization crash box (780 MPa-grade, t=1.8)

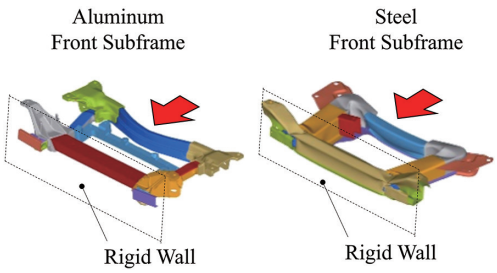

Fig. 20 Subframe crashworthiness evaluation

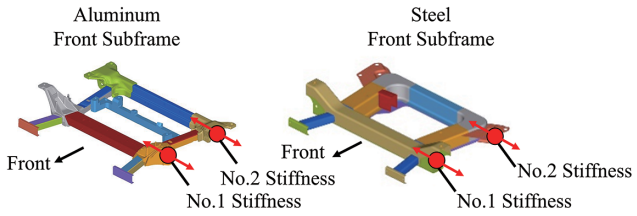

Fig. 21 Comparison of static stiffness of arm attachment (CAE)

Stiffness[17] was calculated using static stiffness analysis (**Fig. 21**) for the lateral stiffness of the arm support sections at the front and rear of the subframe, confirming static stiffness equal to or greater than that of the aluminum front subframe.

As described above, the collision performance (energy absorption) and static stiffness of the developed front subframe were verified using CAE. The results confirmed that performance equal to or better than the aluminum front subframe used as the basis for comparison was achieved.

4.4 Advantages of the developed structure

The weight of the developed front subframe is equivalent to that of the aluminum front subframe. This weight reduction was achieved by thinning and lightening each component through the use of GA980-grade EA steel sheet.

The number of parts is 17, which is below the benchmark result (average of 25 parts from five vehicle models) for the aluminum front subframe.

Furthermore, weld length was reduced by: ①–② integrating components and incorporating brackets through welding methods; and ③ eliminating the sandwich structure by utilizing steel tubes.

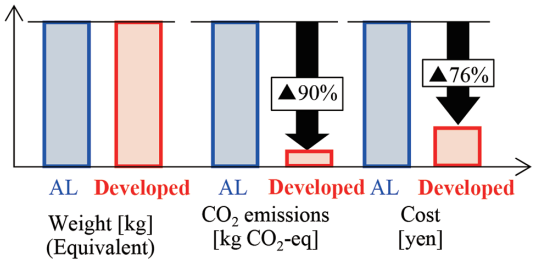

Fig. 22 Comparison of weight, CO_2 emission, cost to aluminum part

Figure 22 shows the advantages of the developed steel subframe over the aluminum subframe in terms of CO_2 emissions in the LCA and part cost. Calculations indicate the developed part achieves equivalent weight to the aluminum part, a 90% reduction in CO_2 emissions, and a 76% reduction in part cost.

This initiative significantly integrated components by applying Nippon Steel's proprietary forming methods to each part. This enabled the development of a front subframe characterized by light weight, fewer parts, and reduced weld length.

5. Conclusion

Steel materials have long been widely utilized in automotive bodies due to their excellent recyclability, formability, and weldability. Among these, high-strength steel sheets are expected to achieve even greater strength in electric vehicle (EV) chassis components, driven by the need for weight reduction and cost efficiency.

This report presents solution technologies for realizing chassis components that deliver advantages in part weight, cost, and CO_2 emissions from a life cycle assessment (LCA) perspective. It describes the development of a front lower arm and a subframe that satisfy EV component requirements while achieving weight equivalent to aluminum. In addition, it introduces the development of a steel tube trailing arm component, which offers lower cost compared to conventional steel tube forming methods, thereby accommodating increased battery capacity.

Looking ahead, we will continue to advance solution technologies that maximize the potential of steel materials, while promoting chassis component development and elemental technology innovation toward the realization of NSafe™-AutoConcept ECO³.

References

1) Kubo, M. et al.: Proceedings of the 2022 Spring Conference of the Society of Automotive Engineers of Japan. Document No. 20225281 (2022)
2) Yoshida, H. et al.: Shinnittetsu Giho. (393), 18–24 (2012)
3) Abe, Y. et al.: Journal of the Japan Society for Technology of Plasticity. 52 (604), 569–573 (2011)
4) Ito, Y. et al.: Proceedings of the 67th Joint Conference on Plastic Processing. 321 (2016)
5) Niwa, T. et al.: Transactions of Society of Automotive Engineers of Japan. 44 (5), 1249–1254 (2013)
6) Bridgman, P.W.: Studies in Large Plastic Flow and Fracture. McGraw-Hill Book Co. New York, 1952
7) Wada, M.: Plastos. 8 (87), 111–115 (2025)
8) Mizumura, M.: Plastos. 2 (16), 186–191 (2019)
9) Tamura, S. et al.: Proceedings of the 67th Joint Conference on Plastic Processing. 69 (2016)
10) Kawachi, T. et al.: Nippon Seitetsu Giho. (412), 97–102 (2019)

11) Onishi, M. et al.: Nissan Technical Review. (90), 19 (2024)
12) Tanaka, Y. et al.: Proceedings of the 69th Joint Conference on Plastic Processing. 247 (2018)
13) Tanaka, Y., Natori, J.: Proceedings of the 2021 Autumn Conference of the Society of Automotive Engineers of Japan. Document No. 20216079 (2021)
14) Tanaka, Y. et al.: Plastos. 6 (72), 725–729 (2023)
15) Tanaka, Y. et al.: Journal of the Japan Society for Technology of Plasticity. 60 (705), 283–288 (2019)
16) Tanaka, Y. et al.: Proceedings of the 2018 Spring Conference on Plastic Processing. 235 (2018)
17) Ohtsuka, K. et al.: Transactions of the Society of Automotive Engineers of Japan. 43 (5), 1087–1092 (2012)

Kenichiro OHTSUKA
Senior Manager, Head of Section
Integrated Steel-Solution Research Lab.-I
Steel Research Laboratories
20-1 Shintomi, Futtsu City, Chiba Pref. 293-8511

Eiji ISOGAI
Senior Manager
Quality Management Div.
East Nippon Works

Manabu WADA
Senior Manager, Head of Section
Nagoya R & D Lab.

Hikaru YUZAWA
Quality Management Div.
Nagoya Works

Ryo URUSHIBATA
Researcher
Integrated Steel-Solution Research Lab.-I
Steel Research Laboratories

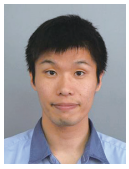

Ryo TABATA
Manager
Quality Management Div.
Nagoya Works

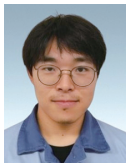

Yuki KITAHARA
Integrated Steel-Solution Research Lab.-I
Steel Research Laboratories

Ryoya YAMAOKA
Integrated Steel-Solution Research Lab.-I
Steel Research Laboratories